J Appl Electrochem (2009) 39:1683–1693
DOI 10.1007/s10800-009-9861-y

ORIGINAL PAPER

Electrolytic magnesium recovery from drinking water membrane residuals

Krishnakumar Raman · John J. Lenhart

Received: 30 July 2008 / Accepted: 4 March 2009 / Published online: 13 March 2009

Abstract The application of advanced membrane processes for drinking water treatment is hampered by the management of the concentrated membrane residuals. This byproduct is typically treated as waste, with the associated costs for disposal. In this study we tested electrolysis as an approach to recover potentially useful products from this waste stream, mitigating its cost of disposal. Aqueous solutions of $Mg(NO_3)_2$, $MgCl_2$, or $MgSO_4$ similar in concentration to those measured in typical membrane concentrates were utilized as test solutions. Cathodic reduction of these solutions resulted in the deposition of brucite, $Mg(OH)_2$, coatings on the surface of the carbon electrode. Recovery was tested in potentiostatic and galvanostatic modes as a function of process parameters and solution composition. Recovery was observed to increase with time, applied voltage, and cell current. The mass deposited also depended upon the electrolyte anion, with under the conditions studied solutions of $MgCl_2$ being the most amenable to electrolysis.

Keywords Electrolysis · Cathodic reduction · Membrane concentrate · Brucite

K. Raman · J. J. Lenhart (✉)
Department of Civil and Environmental Engineering and Geodetic Science, The Ohio State University, Columbus, OH 43210, USA
e-mail: lenhart.49@osu.edu

Present Address:
K. Raman
Malcolm Pirnie, Inc., 1900 Polaris Parkway, Suite 200, Columbus, OH 43240, USA

1 Introduction

Our water supplies face an increasingly heavy burden as human population continues to expand, industrialization increases, and irrigation is implemented on a more widespread basis [1]. To alleviate such unsustainable pressures, many have by necessity resorted to source waters of poor quality (e.g., brackish or saline water). Such water is readily made potable using membrane filtration [2, 3] and consequently over the last two decades the number of water treatment facilities using membrane filtration has dramatically increased [4, 5]. Membrane technologies have issues that hinder their implementation, however, particularly with regard to fouling or scaling, and the management of considerable volumes of concentrated membrane residual [6]. Membrane scaling and fouling have received considerable research focus [7, 8] that has produced process design criteria as well as technical anti-scaling and anti-fouling approaches to mitigate the problems [3, 9, 10]. Similar progress has not been made in improving the management of membrane residuals [5, 6].

The volume of saline residual produced during membrane filtration can be considerable. Depending upon the system utilized and source water quality the reject flow is typically 10–60% of the feed flow and its dissolved solids content may vary from a few thousand parts per million (ppm) to tens of thousands of ppm [5]. Constituents within the membrane concentrate depend on feed water quality, type of membrane process, and degree of fouling/scaling/pre-treatment chemicals added, but are typically dominated by dissolved species such as Na^+, Cl^-, NO_3^- and the hardness cations Ca^{2+} and Mg^{2+} [2, 5]. The U.S. Environmental Protection Agency categorizes membrane reject as an "industrial waste" and disposal regulations are becoming increasingly stringent [2]. Approaches to

manage these membrane residuals can be classified into three general categories: direct discharge techniques, confinement techniques, and land application [5, 6]. Many factors influence the selection of a reject disposal option including, but not limited to: costs, regulatory requirements, reject quantity and quality (composition and constituents), receiving site availability and location, public acceptance, and imminent expansion. But, in most respects the existing management approaches treat the residuals as a waste stream to be disposed [4–6]. The development of alternative approaches to handle membrane residuals from drinking water treatment plants is a necessary step to ensure our future drinking water needs are met. An approach that can recover potentially useful and marketable products would seem particularly attractive.

Electrolysis is a process that can induce chemical changes in an aqueous electrolyte using electricity. Diffusion and advection impact species movement in an electrolytic reactor, but upon passing direct current between the electrodes of an electrolytic cell ion migration in the applied field also occurs. Cations in the solution will migrate towards the negatively-charged cathode and at the same time anions will migrate to the positively-charged anode. Upon reaching the respective electrodes, the ions are discharged via reduction and oxidation reactions, respectively. Efficient and economical electrochemical processes have been used in industry for decades for applications such as electroplating and chlor-alkali synthesis [11]. Of late, electrochemistry has been employed as a technique to treat various waste streams [12–18]. Metals such as copper, nickel and cadmium have been readily electrodeposited from various aqueous waste streams [12–17]. Cathodic reduction and decolorization of nanofiltration concentrate containing azo dyes from textile and printing waste has also been tested [19], with a color reduction of 60–80% being reported.

Metal hydroxide synthesis by electro-generation of base from aqueous solutions has also been attempted. Huang [20], for instance, conducted potentiostatic electrolysis of a 0.75 mM Ca^{2+} solution with NH_4NO_3 as the supporting electrolyte and observed $Ca(OH)_2$ deposition onto the carbon electrode. The amount of $Ca(OH)_2$ deposition increased linearly from 23% to 62% in 20 min under the conditions investigated. Therese and Kamath [21] synthesized $Mg(OH)_2$ by the galvanostatic electrolysis of 0.25 M magnesium chloride and magnesium nitrate solutions. They observed 50% greater $Mg(OH)_2$ yield from magnesium chloride solution than that from magnesium nitrate solution with the same molar concentration and attributed the difference to the significance of hydrogen evolution reaction in the electro-generation of base. Dinamani and Kamath [22] investigated the effect of time, electrolyte concentration and current on the galvanostatic recovery of brucite ($Mg(OH)_2$) from $Mg(NO_3)_2$ solutions. Under the conditions studied, brucite yield increased with time (from 0 to 11.3 mg in an hour) and it almost tripled with a seven fold increase in current [22]. These results suggest that electrochemistry may lead to the recovery of valuable products from membrane reject or possibly a mitigation of its hazard.

We report the results of the electrolytic treatment of synthetic membrane reject solutions. The viability of safe disposal or reuse of the electrolyzed effluent and the effect of process parameter variation on process performance was evaluated using a three electrode bench-scale electrochemical reactor. Aqueous solutions of $Mg(NO_3)_2$, $MgCl_2$ and $MgSO_4$ were used as surrogates for synthetic membrane reject. Electrolysis was conducted using graphite working and counter electrodes and a saturated calomel electrode as the reference electrode. Process parameters examined include system conditions (time of electrolysis, the applied potential difference between the working and reference electrodes, inter electrode distance (IED), and cell current) and solution composition (electrolyte concentration and initial pH). The effect of process mode on deposit morphology was also investigated. As expected, magnesium removal increased with time, applied voltage, and cell current. The mass deposited also depended upon the electrolyte anion, with solutions of $MgCl_2$ being the most amenable to electrolysis.

2 Materials and methods

ACS certified high purity chemicals ($Mg(NO_3)_2 \cdot 2H_2O$, $MgCl_2 \cdot 6H_2O$, $MgSO_4$, and $NaHCO_3$) purchased from Fisher Scientific were used in this study. Stock solutions and standards were prepared by dissolving the appropriate quantity of the required chemical in deionized water (18.2 MΩ-cm, Milli-Q Plus, Millipore) followed by vacuum filtration using a 0.45 micron non-sterile mixed cellulose membrane filter (Fisher Scientific). All labware was acid washed using 10% HNO_3 or 10% HCl (prepared by diluting trace metal grade HNO_3 or HCl from Fisher Scientific) and thoroughly rinsed with deionized water before use.

2.1 Electrolytic experiments

All experiments can be broadly categorized as either potentiostatic or galvanostatic. In potentiostatic mode, the applied potential difference between the working and reference electrodes was fixed at a set value and the cell current varied with time. In galvanostatic mode, the current flowing between the working and counter electrodes was fixed while the potential difference between the working and reference electrodes varied with time.

Experiments conducted in potentiostatic mode evaluated the influence of system parameters (time of electrolysis, applied voltage and IED) and solution composition (electrolyte concentration and initial pH) on magnesium removal using $Mg(NO_3)_2$ and $MgCl_2$ solutions. A series of similar experiments were conducted in galvanostatic mode with the same objective using $Mg(NO_3)_2$ and $MgSO_4$ solutions. Our preliminary experiments indicated that results may be captured effectively in potentiostatic mode at a potential difference of −4 V and in galvanostatic mode at a current rating of 25 mA (equal to a current density of 2.5 mA/cm^2). Hence most of the experiments were conducted at these conditions. In Table 1 we have listed a complete summary of the experimental conditions for the experiments with solutions of $Mg(NO_3)_2$. A parallel suite of experiments were also conducted with solutions comprised of $MgSO_4$ and $MgCl_2$ under essentially identical conditions. Details of these solutions are not listed, however. Note that experiments 1–5 correspond to experiments conducted in potentiostatic mode and experiments 6–8 were those conducted in galvanostatic mode.

All experiments were conducted in a 1.4 L rectangular HDPE reactor using the three electrode VersaStat II system (Princeton Applied Research/AMETEK). Princeton Applied Research's saturated calomel electrode (SCE) was used as the reference electrode. A second SCE (Fisher Scientific) was used to ensure the accuracy of the SCE from Princeton Applied Research. Inert graphite bars (McMaster Carr) with an effective surface area of 10 cm^2 served as both the working and counter electrode. Working and counter electrodes were clamped to a holder to fix the IED at 7 cm for all experiments excluding those elucidating the effect of inter electrode distance. The SCE was placed in close proximity of the working electrode using an articulated electrode holder. Prior to each experiment, the working and counter electrodes were acid washed, rinsed with de-ionized water, and dried at 100 ± 5 °C for 12 h.

An initial suite of experiments were conducted with 500 mL of synthetic membrane reject with typical membrane reject total dissolved solids (TDS) concentration of 2,500–10,000 mg/L and circumneutral pH (data not presented). $Mg(OH)_2$ precipitation was visually observed, however, at these concentrations the dilution needed to bring the samples into the range necessary for Mg measurement introduced excessive errors. Hence, the data reported here were for experiments conducted at lower TDS levels (500–2,500 mg/L). Electrolyte pH was adjusted to a nominal value of 7.3 ± 0.2 using sodium bicarbonate. For experiments at variable pH, 0.01 N NaOH and 0.01 N HNO_3 were used to fix the solution pH. Upon reaching a stable initial pH, the solutions were electrolyzed for a set period of time under the conditions listed in Table 1. The electrolyzed solution was decanted at the conclusion of the experiment and subjected to vacuum filtration. The filtrate was homogenized by stirring, its pH was measured and it was then analyzed for Mg content. Precipitate flakes dislodged from the electrode surface into the solution during electrolysis over long periods of time. These flakes were collected from the solution during vacuum filtration and dried. The working electrode was dried at 100 ± 5 °C for 12 h. After drying, the adhered deposit was dislodged by gentle scraping with a stainless steel blade. This process tended to also dislodge a small portion of the graphite electrode surface. The deposit removed from the electrode was mixed with the dried flakes isolated from the solution, and analyzed to determine composition and morphology using X-ray diffraction (XRD) and scanning electron microscopy (SEM). Most experiments were either duplicated or triplicated.

2.2 Analytical methods

Magnesium concentration was measured by inductively coupled plasma atomic emission spectroscopy (ICP-AES) using Varian's Simultaneous ICP-AES unit as operated by the VISTA software. As the sample magnesium concentration was well above the ceiling limits of the ICP instrument, the samples were suitably diluted. A standard

Table 1 List of experimental conditions

Exp.	Initial Conc. (mg/L)	Time (h)	Initial pH	IED (cm)	Voltage (V)/Current (mA)[a]
1	1,000	1–8.25	7.3 ± 0.2	7	−4
2	2,500	1	7.3 ± 0.2	7	−2, −4, −6, −8
3	1,000	1	7.3 ± 0.2	7–14	−4
4	1,000–2,500	1	7.3 ± 0.2	7	−4
5	2,500	1	5.6–8.3	7	−4
6	1,000	1–18	7.3 ± 0.2	7	25
7	1,000	1	7.3 ± 0.2	7	15–40
8	1,000–2,500	1	7.3 ± 0.2	7	25

[a] The current density for an effective electrode surface area of 10 cm^2 ranged from 1.5 to 4.0 mA/cm^2

reference material solution for magnesium concentration calibration was purchased from Inorganic Ventures Inc. Trace metal grade HNO_3 (Fisher Scientific), diluted to 5%, was used for ICP analysis standard and sample preparation to minimize the possibility of metal precipitation. Four calibration standards of suitable magnesium concentration were utilized. Drift correction was employed using a continuous calibration verification (CCV) standard during runs with more than 10 samples. After the analysis of every tenth sample, CCV was employed. The phases resident within the cathode deposit were evaluated by X-ray diffraction using a Phillips Analytical diffractometer with a copper anode at 35 kV and 20 mA. Data were collected with both a fixed slit and a variable slit goniometer. This slit change does not interfere with the determination of chemical identity. The XRD pattern was processed using JADE 3.0 software. Deposit morphology was investigated after gold coating the precipitate particles attached to a graphite mount using scanning electron microscopy (Quanta 200, FEI Inc.).

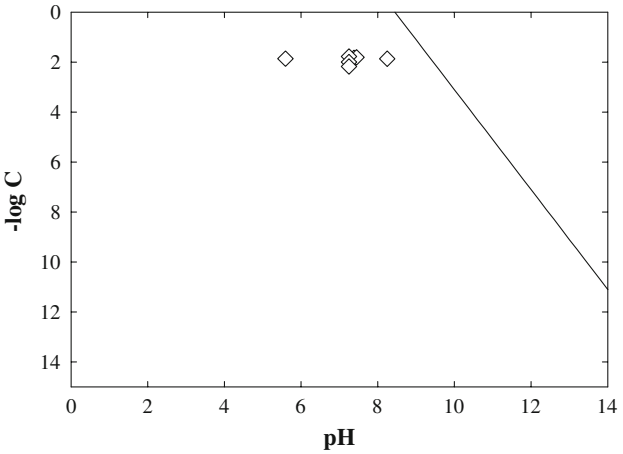

Fig. 1 Comparison of the initial dissolved Mg concentration to that calculated for the solubility of crystalline brucite, $Mg(OH)_2$. The *solid line* designates expected Mg concentration (−log C) with pH as constrained by the solubility product (K_{so}) for brucite of $10^{-11.1}$ [23]. The *open diamonds* represent experimental Mg concentrations corresponding to 2,500, 2,000, 1,500 and 1,000 mg/L $Mg(NO_3)_2$ solutions

3 Results and discussion

Experiments were conducted in systems comprised of aqueous solutions of $Mg(NO_3)_2$, $MgCl_2$ and $MgSO_4$, however, we will focus in this paper on results for the $Mg(NO_3)_2$ systems. Results for the $MgCl_2$ and $MgSO_4$ will be briefly discussed as they compare to those observed for the $Mg(NO_3)_2$ systems. Experiments with $Mg(NO_3)_2$ solutions were conducted in both potentiostatic and galvanostatic modes, whereas $MgCl_2$ and $MgSO_4$ solutions were evaluated only in potentiostatic and galvanostatic modes, respectively.

We compared the initial Mg concentration in the experimental systems to that prescribed by the dissolution of crystalline brucite (Fig. 1). From these calculations, it was evident that all systems were under saturated with respect to $Mg(OH)_2$ and thus any subsequent precipitate formation was due to shifts in the activity of the pertinent species. The stability of Mg solids other than brucite was further evaluated using Visual MINTEQ (Version 2.5), which is free and available for download (http://www.lwr.kth.se/English/OurSoftware/vminteq/). These simulations (not shown) identify in addition to brucite the minerals magnesite ($MgCO_3$), hydromagnesite ($Mg_5(CO_3)_4(OH)_2 \cdot C6H_2O$), periclase (MgO), $Mg_2(OH)_3Cl \cdot 4H_2O$ and artinite ($Mg_2(CO_3)(OH)_2 \cdot 5H_2O$) as thermodynamically favorable solids. In fact, the saturation index for brucite precipitation exceeded that of the other possible mineral phases only at pH values above 12–13. At these elevated pH values, however, observed deviations from electro-neutrality were observed in the calculations, suggesting additional reactions or processes that alter speciation at elevated pH values, particularly those in vicinity of the working electrode, were neglected in the model. These simulations also were based on thermodynamic equilibrium and thus while they may provide an approximation for the bulk system composition they do not account for the potential strong influence of reaction kinetics on chemical speciation in aquatic systems [23].

3.1 Potentiostatic experiments with $Mg(NO_3)_2$

3.1.1 The effect of system conditions

The change in magnesium concentration and solution pH with time during the potentiostatic electrolysis of a 1,000 mg/L $Mg(NO_3)_2$ solution is elucidated in Fig. 2. Additional details of the system conditions for this experiment (Exp. 1) and all others are summarized in Table 1. Over the 8-h time period examined the concentration of magnesium in the solution decreased by approximately 22% from an initial value of 150–120 mg/L. The bulk solution pH was also observed to decrease, falling from an initial value of 7.5 to a final value of 2.7. Concurrent with the changes in solution composition a white precipitate was observed to form on the cathode surface. Over time, portions of the deposit detached from the electrode and settled at the bottom of the reactor.

Although traces of graphite resulting from the removal of the deposit from the electrode were noted, analysis of the deposit with X-ray diffraction produced a well defined pattern consistent with that for crystalline brucite. No other

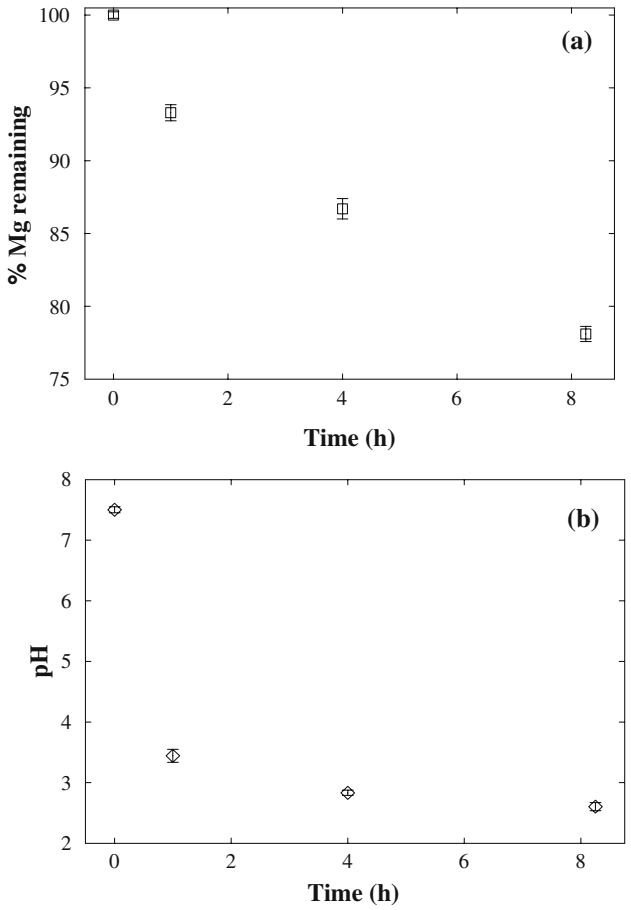

Fig. 2 Results for Exp. 1 (see Table 1) depicted as **a** the percent magnesium remaining in solution and **b** solution pH for a potentiostatically electrolyzed $Mg(NO_3)_2$ solution as function of electrolysis time

magnesium solids were detected. This result, in conjunction with the MINTEQ analyses, suggests the pH in the vicinity of the working electrode likely exceeded 12 as solids other than brucite should be present if the pH in the micro-environment near the electrode surface was lower. High resolution SEM images of the dry deposit depict a sample with a heterogeneous surface with evidence for some porosity (Fig. 3). This differs somewhat from the flake-like morphology observed by Dinamani and Kamath [22] for the galvanostatic production of brucite on stainless steel, perhaps reflecting a dependence in the deposition mechanism as a function of deposition mode as reported in the literature for metal deposition [24, 25].

At the working electrode, it is reported that hydroxide is produced in nitrate solutions via the reduction of both water and nitrate as follows [22]:

(a) $H_2O + {}^1/_2O_2 + 2e^- \rightarrow 2OH^- \quad E^o = 0.40\ V$

(b) $2H_2O + 2e^- \rightarrow H_2 + 2OH^- \quad E^o = -0.83\ V$

(c) $NO_3{}^- + H_2O + 2e^- \rightarrow NO_2{}^- + 2OH^- \quad E^o = 0.01\ V$

(d) $NO_3{}^- + 7H_2O + 8e^- \rightarrow NH_4{}^+ + 10OH^- \quad E^o = 2.67\ V$

With the passage of time, the hydroxyl ions produced by these reactions combine with Mg^{2+} and $MgOH^+$ ions near the working electrode where they deposit as brucite to produce the observed time-dependent increase in magnesium removal. Although hydroxyl ions generated at the working electrode substantially increase the pH in the surrounding micro-environment, the bulk solution pH substantially decreased (see Fig. 2b) as at the counter electrode the oxidation of water occurs.

(e) $H_2O \rightarrow {}^1/_2O_2 + 2H^+ + 2e^- \quad E^o = -1.23\ V$

The rate of decrease in pH slows as time passes as it was easier to scale from the initially low hydrogen ion activity corresponding to pH 7.5 than it was for the hydrogen ion activity corresponding to a pH of 3.4 observed after 1 h of electrolysis.

Increasing the magnitude of the applied potential difference between the reference and working electrodes from −2 to −8 V (Exp. 2) increased magnesium removal by a factor of approximately 4.5 (Fig. 4a). Current recorded

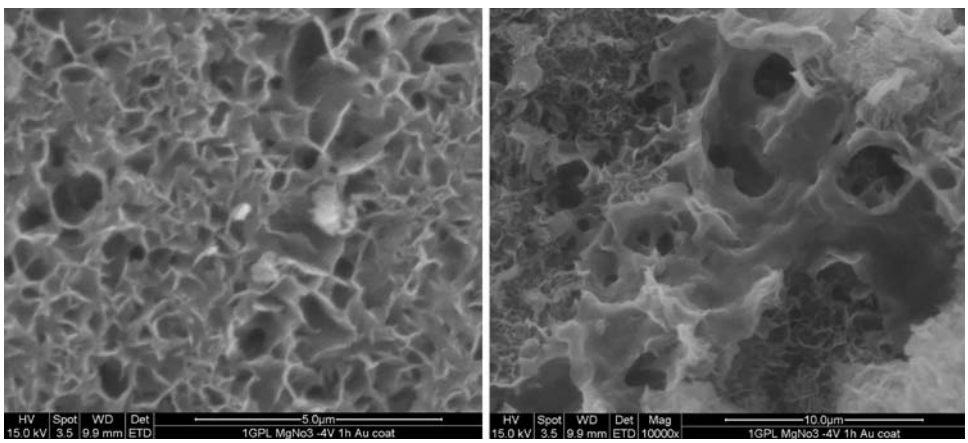

Fig. 3 High resolution SEM micrographs of precipitate from the potentiostatic electrolysis of a $Mg(NO_3)_2$ solution

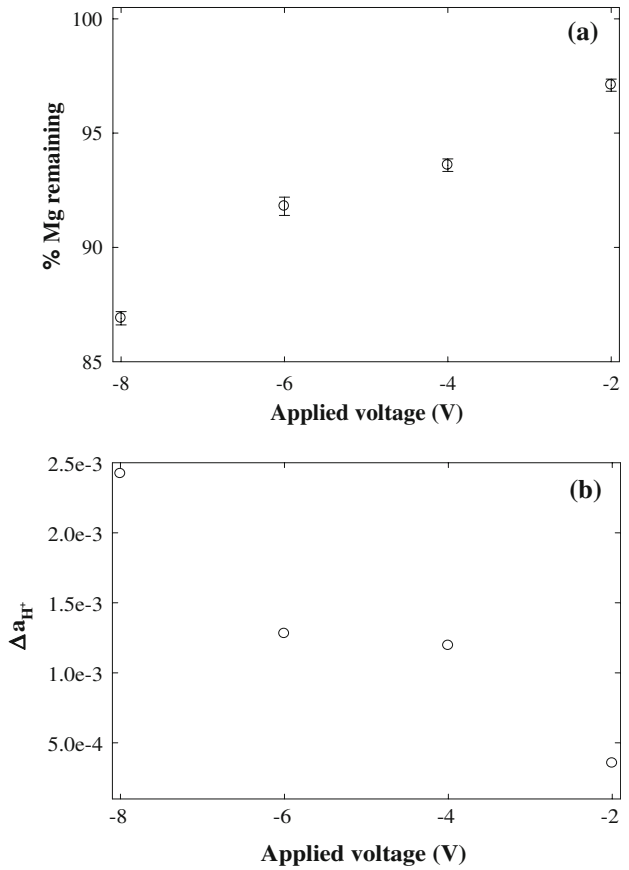

Fig. 4 Results for Exp. 2 (Table 1) shown as **a** the percent magnesium remaining in solution and **b** change in the hydrogen ion activity (Δa_{H^+}) for a potentiostatically electrolyzed $Mg(NO_3)_2$ solution as a function of the applied voltage

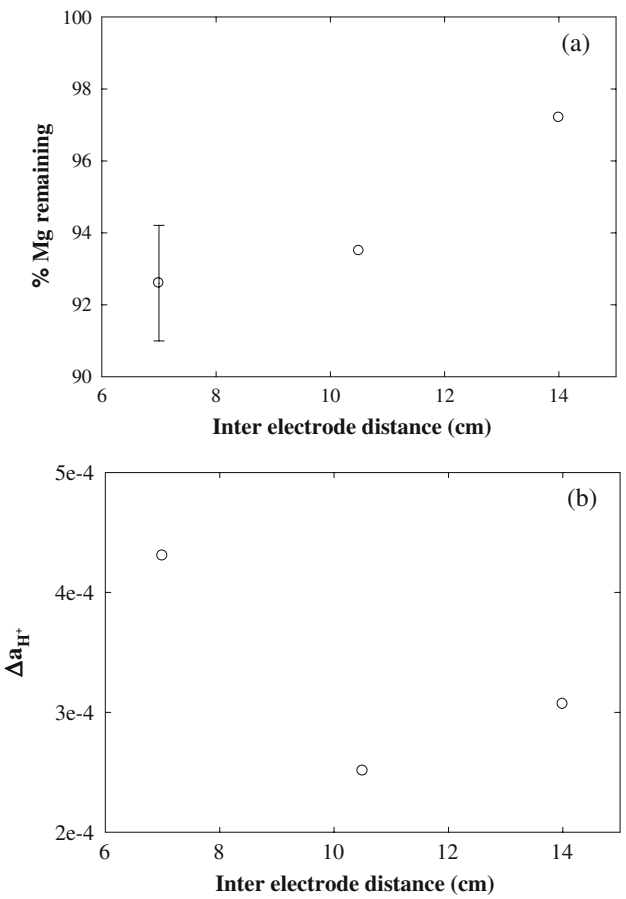

Fig. 5 Results for Exp. 3 (Table 1) represented as **a** the percent magnesium remaining in solution and **b** change in the hydrogen ion activity (Δa_{H^+}) for a potentiostatically electrolyzed $Mg(NO_3)_2$ solution as a function of inter-electrode distance

during these experiments increased with the increase in the magnitude of the applied potential difference, which is consistent with Faradays' law of electrolysis [11].

The difference between the initial hydrogen ion activity and that at the conclusion of each experiment (Δa_{H^+}) as determined from the measured pH values provides an estimate for the net degree of water oxidation. As the magnitude of the applied voltage quadrupled, this difference increased by nearly seven fold (Fig. 4b) as more current and hence greater charge was circulated during a given amount of time. Increasing the magnitude of the applied voltage should improve water and nitrate reduction and thus seems to provide more favorable conditions for brucite precipitation.

Inter-electrode distance can play a significant role in the removal of magnesium. The smaller the inter-electrode distance, the less will be the electrolyte resistance (assuming the system behaves like a conductor whose resistance is directly proportional to the distance between the electrodes) and hence the greater will be the system current and consequently magnesium removal under a given set of conditions. Experiments conducted on systems where the IED was varied from 7 to 14 cm (Exp. 3) provide some evidence in support of this assumption (Fig. 5a). Increasing the IED by a factor of two brought about a concomitant increase in Mg^{2+} concentration. The increase in solution hydrogen ion activity, however, exhibited a similar general trend, but was confounded by an observed increase for an IED of 11 cm that was smaller than that for an IED of 14 cm (Fig. 5b).

3.1.2 The effect of solution composition

Increasing the concentration of $Mg(NO_3)_2$ from 1,000 to 2,500 mg/L as done in Exp. 4 should improve the solution conductivity, thereby increasing the cell current and presumably brucite formation. The results, however, were counter to this expectation as the percent magnesium removal decreased with increasing electrolyte concentration (see Fig. 6a). We were unable to explicitly determine why the expected result was not observed, but perhaps the variance reflected a saturation of the electrode surface and near-electrode area with brucite which consequently

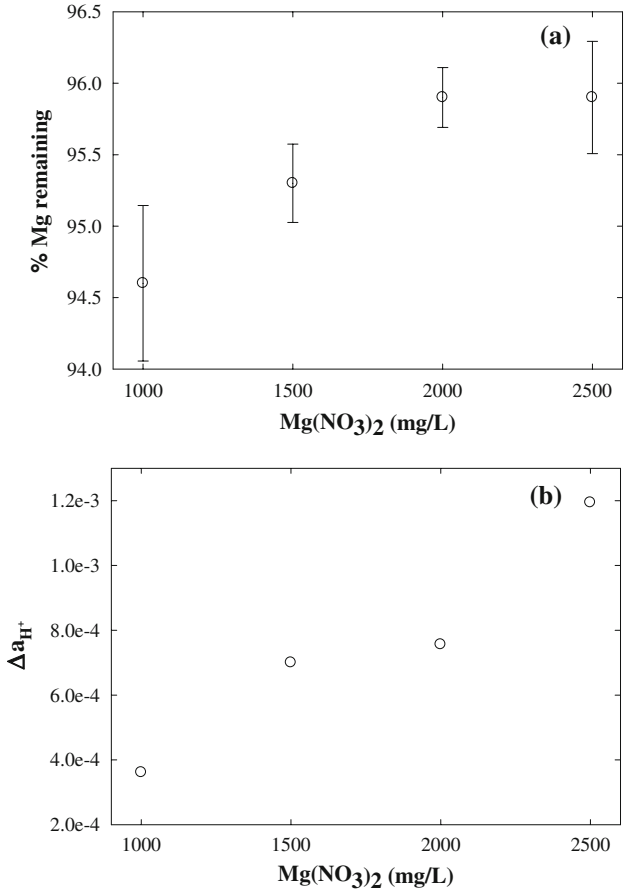

Fig. 6 Results for Exp. 4 (Table 1) portrayed as **a** the percent magnesium remaining in solution and **b** change in the hydrogen ion activity (Δa_{H^+}) in a potentiostatically electrolyzed $Mg(NO_3)_2$ solution as a function of electrolyte concentration

limited additional precipitate formation. Counter to the trend in magnesium concentration the increase in the hydrogen ion activity during electrolyses was observed to scale with the increasing electrolyte concentration (Fig. 6b).

The impact of initial solution pH on magnesium removal was evaluated across an initial pH that ranged from 5.6 to 8.3 (Exp. 5). As the initial pH of the reject solution increases, more OH^- ions should initially be present in the vicinity of the working electrode. This increases the likelihood that the ionic product of brucite will exceed its solubility product, resulting in improved magnesium removal (see Fig. 7). In a similar series of experiments, Therese and Kamath [21] observed that the yield of $Mg(OH)_2$ from a 0.25 M solution comprised of $Mg(NO_3)_2$ electrolyzed galvanostatically increased by a factor of one and a half as the initial electrolyte pH increased from 2 to 4. Interestingly, Therese and Kamath [21] observed little change in removal as the solution pH was further increased to 7. Because Therese and Kamath [21] electrolyzed their solutions galvanostatically these results are not directly

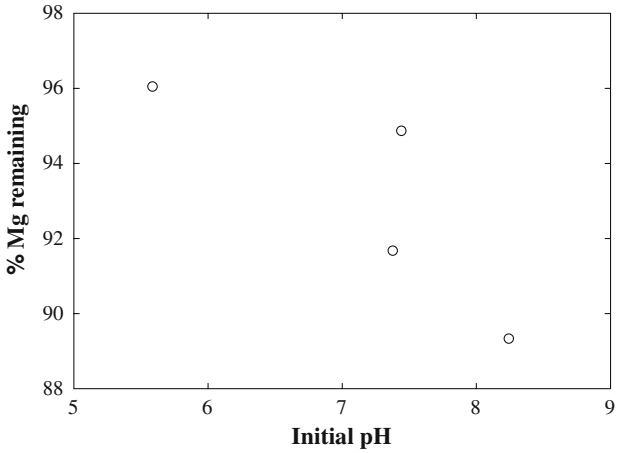

Fig. 7 The percent magnesium remaining in solution in a potentiostatically electrolyzed $Mg(NO_3)_2$ solution as a function of initial solution pH (Exp. 5 in Table 1)

comparable to those presented in Fig. 7, however, the general trend of increasing removal with increasing initial pH remains. Although the increase in initial pH enhanced magnesium removal, it had little impact on the final pH of the system (data not shown).

3.2 Galvanostatic experiments with $Mg(NO_3)_2$

3.2.1 The effect of system conditions

Unlike potentiostatic electrolysis, the rate of electrodeposition is fixed during galvanostatic electrolysis. Hence we anticipate the system to perform differently under galvanostatic conditions. The effect of time on the galvanostatic deposition of $Mg(OH)_2$ from a $Mg(NO_3)_2$ solution from Exp. 6 is depicted in Fig. 8. The solution magnesium concentration and solution pH both exhibited a significant decrease over the first 4 h of electrolysis, followed by a more gradual decrease over the remaining 14 h. Little change was observed after 8 h, however, which matches our observations under potentiostatic conditions (Fig. 2). Evaluation of experimental kinetics (analysis not shown) indicates that magnesium removal follows the Monod function, i.e., Mg removal increases linearly with time up to a certain point of time and changes little thereafter. This suggests the available area on the electrode surface for brucite deposition may have become saturated or that the concentration of solute ions necessary for solid formation in the vicinity of electrode may have been depleted. Alternatively, the deposit detached during the experiment could have dissolved in the acidic electrolyte. Over a smaller time scale of 1 h, Dinamani and Kamath [22] observed a linear decrease in magnesium concentration from a solution comprised of 0.1 M $Mg(NO_3)_2$ electrolyzed galvanostatically. Unfortunately, Dinamani and Kamath [22] did not present results over longer

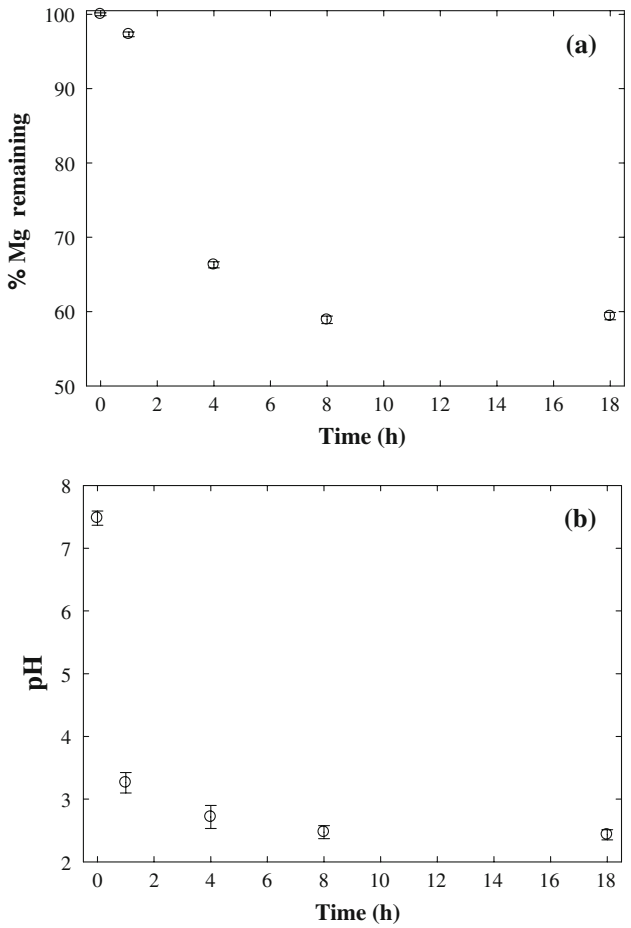

Fig. 8 Results for Exp. 6 (Table 1) shown as **a** the percent magnesium remaining in solution and **b** solution pH for a galvanostatically electrolyzed $Mg(NO_3)_2$ solution as a function of electrolysis time

periods of time so it isn't known whether their results exhibited similar long-term removal tendencies. SEM micrographs (Fig. 9) of the 18 h precipitate provide a morphology that was flakier in nature than that observed from the potentiostatic experiments (see Fig. 3). Kamath and coworkers [21, 22] also observed a similar flaky precipitate under galvanostatic conditions. This difference may reflect that the mode of deposition under galvanostatic conditions differed from that under potentiostatic conditions. Under galvanostatic conditions deposition is reported to be due to the process of progressive nucleation [24, 25], wherein the precipitate nuclei grow on pre-existing nuclei under a fixed rate of deposition and presumably present a flaky aspect.

Cell current is a very important process parameter and under galvanostatic conditions it is expected that over a given time period that charge circulation, OH^- ion generation and thus $Mg(OH)_2$ precipitation will increase with increasing cell current. Solutions of $Mg(NO_3)_2$ were electrolyzed for 1 h under cell currents of 15–40 mA, corresponding to current densities of 1.5–4.0 mA/cm^2 (Exp. 7), with the results indicating that magnesium removal scales directly with increasing cell current (Fig. 10a). The trend was in fact highly linear ($R^2 = 0.96$), as expected, based on Faradays' law of electrolysis. Similar results have also been reported by Dinamani and Kamath [22] during the galvanostatic electrolysis of 0.1 M $Mg(NO_3)_2$ solution from about 5 to 32 mA. Figure 10b echoes that the change or increase in the solution hydrogen ion activity during electrolysis also increases with cell current, consistent with enhanced water oxidation at the counter electrode.

3.2.2 *The effect of solution composition*

The effect of $Mg(NO_3)_2$ concentration on process performance was also evaluated in galvanostatic mode (Exp. 8). Increasing electrolyte concentration should improve electrolyte conductivity and at a constant cell current enhanced magnesium removal should result. Furthermore, increasing $Mg(NO_3)_2$ concentration increases solution Mg^{2+} concentration and consequently the probability that the ionic product may exceed the solubility product, enhancing

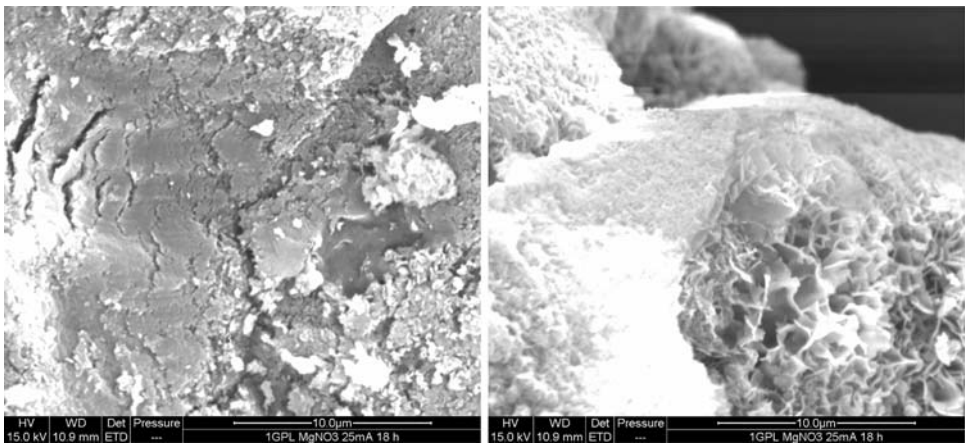

Fig. 9 High resolution SEM micrograph of precipitate from the galvanostatic electrolysis of a $Mg(NO_3)_2$ solution in galvanostatic mode

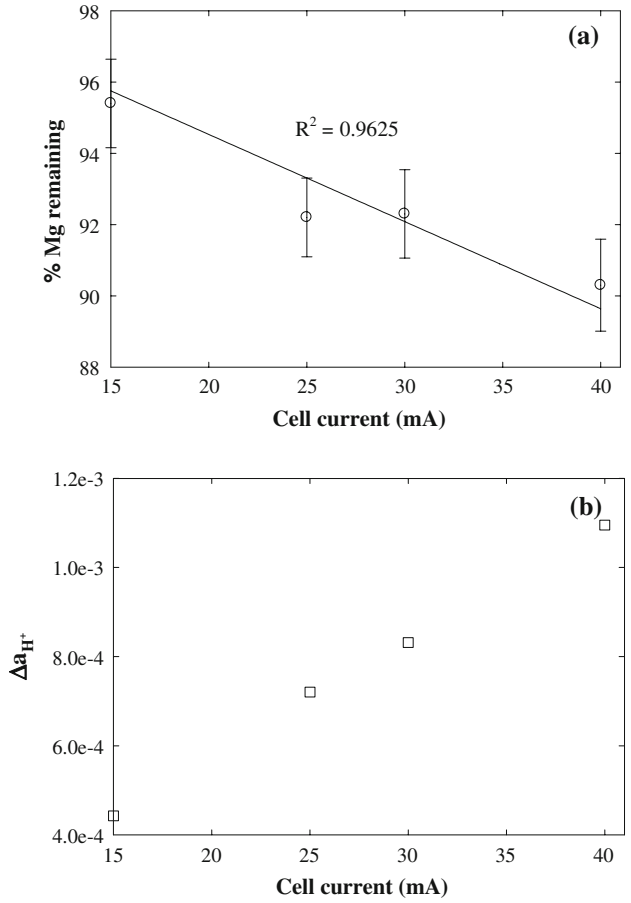

Fig. 10 Results for Exp. 7 (Table 1) depicted as **a** the percent magnesium remaining in solution and **b** change in the hydrogen ion activity (Δa_{H^+}) for a galvanostatically electrolyzed $Mg(NO_3)_2$ solution as a function of cell current

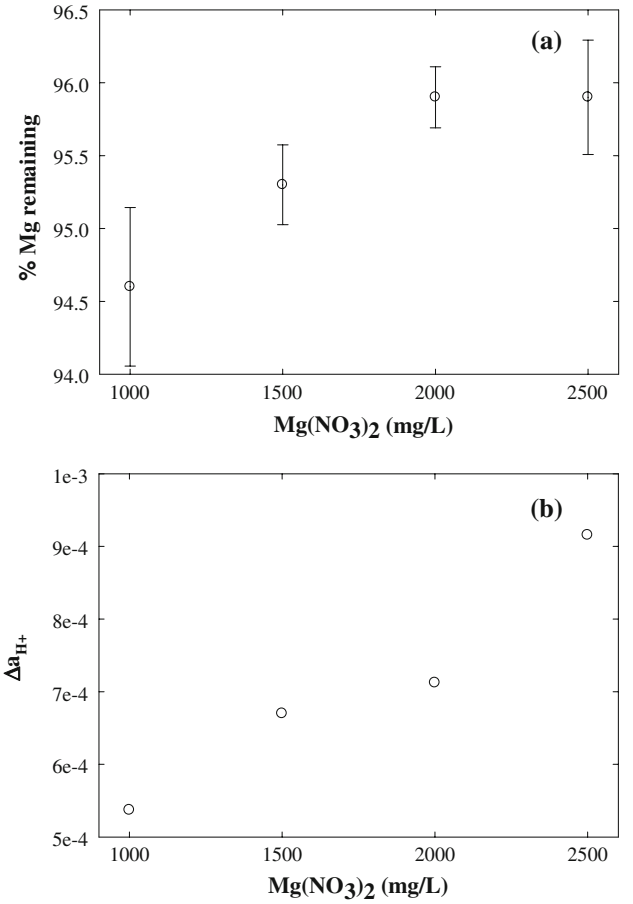

Fig. 11 Results for Exp. 8 (Table 1) shown as **a** the percent magnesium remaining in solution and **b** change in the hydrogen ion activity (Δa_{H^+}) for a galvanostatically electrolyzed $Mg(NO_3)_2$ solution as a function of electrolyte concentration

brucite precipitation even for a fixed OH^- ion concentration in the vicinity of the working electrode. Similar to our potentiostatic experiments, increasing $Mg(NO_3)_2$ concentration did not produce an increase in magnesium removal (Fig. 11a). This again likely reflects a saturation of the electrode. Although the expected trend in magnesium removal with increasing magnesium concentration was not observed, the change in the solution hydrogen ion activity was observed to increase with increasing $Mg(NO_3)_2$ concentration (Fig. 11b).

3.3 Experiments with $MgCl_2$ and $MgSO_4$

The influence of the electrolyte anion was investigated under experimental conditions similar to those presented for $Mg(NO_3)_2$ by electrolyzing solutions comprised of $MgCl_2$ and $MgSO_4$. The $MgCl_2$ solutions were investigated under potentiostatic conditions, versus galvanostatic for the $MgSO_4$ solutions. Because the results of these experiments were very similar to those observed with the $Mg(NO_3)_2$ solutions the experimental data are not presented. Instead, we discuss the results on the basis of how they differ to those previously presented for the $Mg(NO_3)_2$ solutions.

3.3.1 Potentiostatic experiments in $MgCl_2$ systems

The $MgCl_2$ solutions were electrolyzed under potentiostatic conditions as a function of applied voltage, time and concentration. The results mirrored those for $Mg(NO_3)_2$, except that we observed consistently greater magnesium removal (approximately 15–30%) than those achieved under similar conditions in $Mg(NO_3)_2$ solutions. In the absence of nitrate, the hydrogen evolution reaction (reaction b) drives OH^- formation near the working electrode. A greater brucite yield from a $MgCl_2$ solution in comparison to a $Mg(NO_3)_2$ solution under similar conditions could signify the relative importance of hydrogen evolution

reaction over nitrate reduction, as it is the only reaction that occurs in $MgCl_2$ solution [21]. It could also reflect contributions from chlorine evolution occurring at the anode.

(f) $Cl^- \rightarrow {}^1/_2Cl_{2(g)} + 2e^- \quad E^o = -1.36\,V$

This reaction does not release hydrogen ions and thus hydroxyl ions produced by reaction (b) could form brucite more readily. Therese and Kamath [21] observed the $Mg(OH)_2$ yield from a $MgCl_2$ bath was 150% of that from a $Mg(NO_3)_2$ bath of the same molar magnesium concentration. Although the experimental conditions are not directly comparable to ours (Therese and Kamath [21] used different electrodes and a higher Mg^{2+} concentration), these results do demonstrate the relative importance of the hydrogen evolution and chlorine evolution reactions.

3.3.2 *Galvanostatic experiments in $MgSO_4$ systems*

Solutions of $MgSO_4$ were electrolyzed under galvanostatic conditions as a function of time, applied current, and concentration. Trends in magnesium removal from the sulfate solutions were again similar to those for the nitrate system except that Mg removal was much lower (by nearly 80%) than those measured from $Mg(NO_3)_2$ solutions under similar operating conditions. In the absence of nitrate, sulfate reduction can occur as follows [26]

(g) $SO_4{}^{2-} + H_2O + 2e^- \rightarrow SO_3{}^{2-} + 2OH^-$
$E^o = -0.93\,V$

The lower removal thus may indicate the relative importance of nitrate reduction over sulfate reduction as might be expected based up on the standard reduction potentials of these reactions (e.g., compare reactions c and d to g).

4 Conclusions

The technical feasibility of electro-generation of solid magnesium hydroxide from synthetic reject containing $Mg(NO_3)_2$, $MgCl_2$ or $MgSO_4$ was established in this study. $MgCl_2$ solutions had the highest mass yield of solid at a given TDS followed by $Mg(NO_3)_2$, and $MgSO_4$ solutions. Magnesium removal from solution increased with time, the magnitude of the applied potential difference (between the reference and working electrodes), cell current, decreased inter electrode distance, and initial pH of the reject. The effect of electrolyte concentration on magnesium removal was counter to expectations and may reflect the limited electrode surface area for deposition or the dissolution of dislodged deposit. Additional research to optimize the process (e.g., by evaluating higher surface area electrodes or alternative electrode materials) could also provide additional insight into this process.

Brucite was the solid generated under all the conditions investigated, but its morphology depended on the mode of electrolysis. This likely reflects differing modes of deposition, instantaneous nucleation observed under potentiostatic conditions versus progressive nucleation observed under galvanostatic conditions, which could be exploited for morphology specific applications like sensor technology and MgO nano-particle synthesis. In all cases, the resulting electrolyte was acidic regardless of the initial reject pH and thus direct disposal into water resources may not be possible. However, re-use or sale of this acidic solution as well as capture and re-sale of hydrogen evolved during the process may generate additional revenue. Further research is also needed to evaluate this possibility.

Acknowledgements The authors wish to thank the Ohio Water Development Authority for partial support of this research. Additional support to K.R. was provided by The Ohio State University in the form of a University Fellowship.

References

1. United Nations (2006) Water, a shared responsibility: the 2nd United Nations world water development report. UNESCO Publishing, Paris
2. American Water Works Association (1999) Water quality and treatment, 5th edn. McGraw-Hill, New York
3. Crittenden JC, Trussell RR, Hand DW, Howe KJ, Tchobanoglous G (2005) Water treatment: principles and design, 2nd edn. Wiley, New York
4. AWWA Membrane Residuals Management Subcommittee (2003) J Am Water Works Assoc 95:68
5. AWWA Membrane Residuals Management Subcommittee (2004) J Am Water Works Assoc 96:73
6. van der Bruggen B, Lejon L, Vandecasteele C (2003) Environ Sci Technol 37:3733
7. Howe KJ, Clark MM (2002) Environ Sci Technol 36:3571
8. Goosen MFA, Sablani SS, Al-Hinai H, Al-Obeidani S, Al-Belushi R, Jackson D (2004) Sep Sci Technol 39:2261
9. Chen D, Weavers LK, Walker HW, Lenhart JJ (2006) J Memb Sci 276:135
10. Ning RY, Troyer TL, Tominello RS (2005) Desalination 172:1
11. Bagotsky VS (2006) Fundamentals of electrochemistry, 2nd edn. Wiley Interscience, Princeton
12. Yang C-L, Kravets G (2002) Chem Eng Commun 189:827
13. Malkin VP (2002) Chem Petrol Eng 38:619
14. Lupi C, Pasquali M (2003) Miner Eng 16:537
15. Tramontina J, Azambuja DS, Piatnicki CMS (2002) J Braz Chem Soc 13:469
16. Elsherief AE (2003) Electrochim Acta 48:2667
17. Grau JM, Bisang JM (2003) J Chem Technol Biotechnol 78:1032
18. Juttner K, Galla U, Schmieder H (2000) Electrochim Acta 45:2575
19. Bechtold T, Turcanu A (2004) J Appl Electrochem 34:903
20. Huang HJ (1983) J Electrochem Soc 130:630
21. Therese GHA, Kamath PV (1998) J Appl Electrochem 28:539
22. Dinamani M, Vishnu Kamath P (2004) J Appl Electrochem 34:899

23. Morel FMM, Hering JG (1993) Principles and applications of aquatic chemistry. Wiley, New York
24. Manhabosco TM, Englert G, Muller IL (2006) Surf Coat Technol 200:5203
25. Michel S, Diliberto S, Boulanger C, Stein N, Lecuire JM (2005) J Crystal Growth 277:274
26. CRC Press (1990) In Lide DR (ed) CRC handbook of chemistry and physics, 71st edn. CRC Press, Boston